Experimental evaluation of a R134a/CO_2 cascade refrigeration plant

Carlos Sanz-Kock[1], Rodrigo Llopis[1,*], Daniel Sánchez[1], Ramón Cabello[1], Enrique Torrella[2]

[1]Jaume I University, Dep. of Mechanical Engineering and Construction, Campus de Riu Sec s/n E-12071, Castellón, Spain

[2] Polytechnic University of Valencia, Department of Applied Thermodynamics, Camino de Vera, 14, E-46022, Valencia, Spain

*Corresponding author: R. Llopis (rllopis@uji.es), Phone: +34 964 72 8136; Fax: +34 964 728106.

ABSTRACT

We present the experimental evaluation of a R134a/CO_2 cascade refrigeration plant designed for low evaporation temperature in commercial refrigeration applications. The test bench incorporates two single-stage vapour compression cycles driven by semi hermetic compressors coupled thermally through two brazed plate cascade heat exchangers working in parallel and controlled by electronic expansion valves. The experimental evaluation (45 steady-states) covers evaporating temperatures from -40 to -30ºC and condensing from 30 to 50ºC. In each steady-state, we conducted a sweep of the condensing temperature of the low temperature cycle with speed variation of the high temperature compressor. Here, the energy performance of the plant is analysed, focusing on the compressors' performance, temperature difference in the cascade heat exchanger, cooling capacity, COP and compressors discharge temperatures.

KEYWORDS

cascade; two-stage; low GWP; R134a; carbon dioxide; energy efficiency

NOMENCLATURE

COP	coefficient of performance
c_p	specific isobaric heat, kJ·kg^{-1}·K^{-1}
GWP	global warming potential (100 years integration)
h	specific enthalpy, kJ·kg^{-1}
HT	high temperature cycle
LT	low temperature cycle
$\dot{m}$	mass flow rate, kg·s^{-1}
N	compressor's speed, rpm
P	pressure, bar
P_C	compressor power consumption, kW
P_{gc}	gas-cooler power consumption, kW
$\dot{Q}$	heat transfer rate, kW
SF	secondary fluid
t	compression ratio
T	temperature, ºC
$\dot{V}$	volumetric flow rate, m^3·h^{-1}
w_s	isentropic specific compression work, kJ·kg^{-1}
x_v	vapour title

GREEK SYMBOLS

η_G	compressor global efficiency
Δ	increment
ρ	density, kg·m^{-3}

SUBSCRIPTS

C1	cascade heat exchanger number 1
C2	cascade heat exchanger number 2
casc	cascade
dis	discharge
env	environment
exp	expansion

gc	gas-cooler
H	high-temperature cycle
i	inlet
K	condensing level
L	low-temperature cycle
o	output
O	evaporating level
ref	refrigerant
res	receiver
s	isentropic
sf	secondary fluid in LT evaporator (water-tyfoxit)
suc	suction
w	secondary fluid in HT condenser (water)

1. Introduction

The high warming impact associated to refrigeration systems, due to the direct leakage of refrigerants and to the indirect emissions of CO_2 by electricity consumption, moves scientific community and institutions to more environmental friendly solutions. Among refrigeration groups, centralized commercial refrigeration highlights because of its high annual leakage rate, commonly higher than 10% of the total charge of the system [1] and because of its high energy consumption [2]. Both negative aspects motivated European Commission to approve the revision of the F-Gas regulation [3], focusing the efforts on reducing the emissions to the atmosphere of greenhouse refrigerants. The agreements that most affect centralized commercial refrigeration in Europe are: from 2020 on refilling of systems with refrigerants of GWP>2500 will not be allowed if the total equivalent charge of the system overcomes 40 tonnes of equivalent CO_2; from 2022 in centralized commercial refrigeration systems with capacity of more than 40kW, refrigerants with GWP$\geq$150 will not be permitted except for the primary refrigerant of cascade systems, where refrigerants with GWP up to 1500 will be allowed. Both agreements represent the future disappearance of the most used refrigerants in centralized commercial refrigeration at low temperature in Europe [4], the R404A and the R507A with GWP of 3700 and 3800, respectively [5]. Commercial refrigeration section, specially supermarkets, needs to adapt their refrigeration systems and fluids to the new F-Gas regulation. The adaptation will be based on low GWP refrigerants, and generally it would need to replace the common single-stage refrigeration systems by new refrigeration configurations adapted to the new fluids. The system that now attract more attention is cascade refrigeration using CO_2 as LT refrigerant, although different refrigerant options are considered for the HT cycle.

In literature, the most analysed cascade refrigeration system is the combination NH_3/CO_2. For this pair, Lee et al. [6] evaluated theoretically the optimal condensing temperature of the cascade heat exchanger and the COP for evaporating levels between -45 and -55 ºC. Dopazo et al. [7], also theoretically, analysed the influence of the cycle parameters on its efficiency and evaluated the optimal condensing temperature, too. Both works presented polynomials to evaluate the optimum condensing level. And finally, Messineo [8] evaluated theoretically the performance of this system regards a direct two-stage R404A system, stating that the cascade system is an interesting alternative in commercial refrigeration for energy, security and environmental reasons. For other combinations of refrigerants, Getu and Bansal [9] analysed theoretically cascades of CO_2 with ammonia, propane, propylene, ethanol and R404A, concluding that the best pair from an energy point of view was ethanol/CO_2 followed by NH_3/CO_2. And, Xiao and Liu [10] studied theoretically the application of R32 as HT refrigerant.

Regarding experimental evaluation of cascade systems, Bingming et al. [11] presented the experimental results of a NH_3/CO_2 cascade driven by two screw compressors for a condensing temperature of 40 ºC and evaporating temperatures between -50 to -30 ºC. They evaluated experimentally the influence of the temperature difference in the cascade heat exchanger, the condensing temperature in the LT cycle and the degree of superheat in this heat exchanger. Also, they presented an experimental comparison with single-stage and two-stage NH_3 systems, concluding that the cascade system is very competitive in low temperature applications, specially below -40 ºC. With reciprocating compressors, Dopazo and Fernández-Seara [12], evaluated the performance of a NH_3/CO_2 cascade for evaporating temperatures between -50 to -35ºC and for a condensing temperature of 30 ºC. They studied experimentally the optimum condensing temperature of the LT cycle and compared the performance of the plant with a direct two-stage NH_3 system, concluding that the cascade better performs for evaporating temperatures below -35 ºC. Finally, da Silva [13] presents a comparison of a R404A/CO_2 cascade with semi hermetic compressors with direct expansion single-stage systems of R404A and R22 in a supermarket application designed for operation at -30 ºC. The study concludes that the cascade can reduce energy consumption between 13 to 24 % respect the single-stage configuration and the refrigerant charge is reduced, however, the investment cost of the cascade is 18.5 % higher. However, they do not present the energy evaluation of the cascade system under different operating conditions.

As can be observed, most part of scientific work deals with theoretical performance evaluation of cascade systems and with establishing their optimum LT condensing conditions. Few experimental works have been reported up to now and most of them deal with NH_3/CO_2 systems for industrial applications, which are not recommended for commercial systems because of security reasons. UNEP [14] promotes the R134a/CO_2 cascade refrigeration systems as a high-security low-GWP solution for centralized commercial refrigeration, especially for supermarkets, and some brands have selected this system as a future solution to overcome the new F-Gas regulation. However, no experimental work exists about this configuration. Therefore, this communication pretends to cover this lack of research and presents the experimental evaluation of R134a/CO_2 cascade refrigeration prototype driven by semi hermetic compressors over a wide range of working conditions.

2. Experimental plant

The experimental plant, which can be appreciated in Figure 1, corresponds to a R134a/CO_2 cascade refrigeration system designed to operate at the low evaporating temperature level of commercial refrigeration (-40 to -30 ºC). The plant is driven by two single-stage reciprocating compressors, the heat exchangers are of brazed plate type and incorporates electronic expansion valves. We present the schematic diagram of the plant, the position of the measurement devices and the designation in Figure 2. Next, we present the details of the plant, of the thermal support system and of the measurement instrumentation.

Figure 1. View of the cascade refrigeration prototype

Figure 2. Schematic diagram of the experimental plant

2.1. Refrigeration cycle

The refrigerating cycle is detailed in Figure 2. It is an indirect two-stage or cascade system composed of two single-stage cycles coupled thermally with two cascade heat exchangers working in parallel, which act as evaporator of the HT cycle and condenser of the LT cycle. We use CO_2 in the LT cycle and R134a in the HT cycle.

2.1.1 LT cycle

A CO_2 variable speed semi hermetic compressor for subcritical applications, with a displacement of 3.48 m^3/h at 1450 rpm and a nominal power of 1.5 kW, drives the LT cycle. The lubricant oil is POE C55E. The compressor absorbs the vapour at the suction point (suc,L) and compresses it to the LT high pressure (dis,L), then we separate the lubricant oil. Following, the refrigerant gets into a gas-cooler (gc,i,L) where the CO_2 is desuperheated with an air cooler heat exchanger before entering to the cascade heat exchangers (gc,o,L), since generally the discharge temperature is higher than the environment temperature. This cross flow heat exchanger, driven at its nominal speed with a fan of 75 W of power consumption, has a heat transfer area of 0.6 m^2 in the refrigerant side and of 3.36 m^2 in the air side. Next, CO_2 flow is divided and condensated it in two plate heat exchangers (C1,i,L and C2,i,L) with a total heat transfer area of 3.52 m^2. CO_2 leaving the condensers (C1,o,L and C2,o,L) is joined and its mass flow rate is measured with a Coriolis mass flow meter ($M_{ref,L}$). Then, it enters to the receiver and feeds the

expansion valve of the cycle (exp,i,L), an electronic expansion valve that controls the evaporating process in a brazed plate evaporator with a heat transfer area of 2.39 m^2. The valve regulates the degree of superheat at the evaporator exit (O,o,L) with a NTC and a pressure gauge. The heat load to the evaporator is provided with a loop working with a tyfoxit-water mixture (84 % by volume) which allows to operate up to -45 ºC. This loop allows regulating the inlet temperature of the SF to the evaporator (sf,i) and varying the SF flow rate (V_{sf}).

2.1.2 High Temperature cycle (HT cycle)

A R134a variable speed semi hermetic compressor, with a displacement of 32.66 m^3/h at 1450 rpm and nominal power of 3.7 kW, drives the single-stage HT cycle. The lubricant oil is POE SL32. The compressor absorbs the superheated refrigerant coming from the cascade heat exchangers (suc,H) and delivers it compressed to the HT high pressure (dis,H). Then, lubricant oil is separated and it feeds the condenser (k,i,H), a brazed plate heat exchanger with a heat transfer area of 2.39 m^2. At the exit of the condenser the HT refrigerant mass flow rate ($M_{ref,H}$) is measured with a coriolis mass flow meter. Then the refrigerant gets into the receiver. Next, the refrigerant feeds two electronic expansion valves (C1,exp,i,H and C2,exp,i,H) that regulate the evaporation process in the two cascade heat exchangers. The valves regulate independently the degree of superheat at the exit of these heat exchangers (C1,O,o,H and C2,O,o,H) with NTC sensors and pressure gauges. Heat rejection in the condenser is performed with a loop working with water, which allows controlling the inlet temperature (w,i) and varying the flow rate (V_w). More information about the secondary loops can be found in the work of Torrella et al. [15] and Llopis et al. [16, 17]

2.2. Measuring system

The experimental plant is fully instrumented to analyse the energy performance of the cycle. The allocation of sensors is presented in Figure 2. It is equipped with 24 T-type immersion thermocouples for measuring refrigerant and secondary fluids temperature and a T-type air thermocouple for the environment one. Pressure is measured with 7 piezoelectric gauges for the LT cycle and 4 for the HT cycle, refrigerant mass flow rates with two Coriolis mass flow meters ($M_{ref,L}$ and $M_{ref,H}$) and secondary volumetric flow rates (V_{sf} and V_w) with electromagnetic flow meters. Power consumption is obtained with two digital watt meters ($P_{c,L}$ and $P_{c,H}$) and the compressors' speed (N_L and N_H) with the signal from the inverter drives, calibrated using accelerometers and a frequency analyzer system. The calibration range and accuracies of the measurement devices are detailed in Table 1.

All the information obtained from the sensors is gathered by a cRIO data acquisition system (24 bits of resolution) and handled online with an own developed application based on LabView [18].

Table 1. Accuracies and calibration range of the transducers

3. Data reduction

The analysis of the experimental plant is based on the information provided by the detailed measurement system. With the measurements, thermodynamic properties of the refrigerants in the cycles are evaluated using Refprop 9.1 database [19].

Phase change temperatures in the heat exchangers are calculated using measured inlet pressure values and considering saturated state. LT evaporating temperature is calculated with (1) using pressure at the inlet of the evaporator, and LT condensing temperature with (2) with pressure at the inlet of the cascade condensers. For the HT, the evaporating temperature is evaluated with (3) using pressure at the inlet of cascade condenser 1, and the condensing level with (4) using the discharge pressure.

$$T_{O,L} = f\left(P = P_{O,i,L}; x_v = 0\,; CO_2\right) \quad (1)$$

$$T_{K,L} = f\left(P = P_{C,i,L}; x_v = 1; CO_2\right) \quad (2)$$

$$T_{O,H} = f\left(P = P_{C1,o,i,H};\ x_v = 0\,; R134a\right) \quad (3)$$

$$T_{K,H} = f\left(P = P_{dis,H};\ x_v = 1\,; R134a\right) \quad (4)$$

Then, the temperature difference in the cascade heat exchanger is computed with (5).

$$\Delta T_{casc} = T_{K,L} - T_{O,H} \quad (5)$$

Equations (6) and (7) represent the pressure ratios of the CO_2 and R134a compressors, respectively.

$$t_L = {P_{dis,L}}\Big/{P_{suc,L}} \quad (6)$$

$$t_H = {P_{dis,H}}/{P_{suc,H}} \tag{7}$$

Regarding compressors' performance, the global efficiencies of the LT and HT compressors are calculated with Equations (8) and (9), respectively, where the specific isentropic compression works are obtained with relations (10) and (11). The compression work is evaluated with the specific enthalpy at compressor inlet and the subsequent isentropic specific enthalpy at discharge.

$$\eta_{G,L} = \dot{m}_{ref,L} \cdot \frac{w_{s,L}}{P_{c,L}} \tag{8}$$

$$\eta_{G,H} = \dot{m}_{ref,H} \cdot \frac{w_{s,H}}{P_{c,H}} \tag{9}$$

$$w_{s,L} = h_{s,L} - h_{suc,L} \tag{10}$$

$$w_{s,H} = h_{s,H} - h_{suc,H} \tag{11}$$

About the energy parameters of the plant, the heat transfer rates in the LT cycle are evaluated as follows: The cooling capacity, which corresponds to the cooling capacity provided by the plant, with Equation (12), considering the expansion process as isenthalpic. Heat rejection at the gas-cooler with Equation (13). Condensation heat transfer in the cascade heat exchanger with Equation (14), where we average the enthalpy difference of both condensers. And the individual refrigerating COP of the LT cycle with Equation (15).

$$\dot{Q}_{O,L} = \dot{m}_{ref,L} \cdot \left(h_{O,o,L} - h_{O,i,L}\right) \tag{12}$$

$$\dot{Q}_{gc,L} = \dot{m}_{ref,L} \cdot \left(h_{gc,i,L} - h_{gc,o,L}\right) \tag{13}$$

$$\dot{Q}_{K,L} = \dot{m}_{ref,L} \cdot \left[\frac{\left(h_{C1,k,i,L} - h_{C1,k,o,L}\right) + \left(h_{C2,k,i,L} - h_{C2,k,o,L}\right)}{2}\right] \tag{14}$$

$$COP_L = \frac{\dot{Q}_{O,L}}{P_{C,L} + P_{gc,L}} \tag{15}$$

Regarding the HT cycle, cooling capacity in the cascade heat exchanger is evaluated with Equation (16), where the specific cooling capacity is the average of the enthalpy difference in both cascade heat exchangers. In this case, the expansion processes are considered isenthalpic too. The heat rejection in

the HT condenser is calculated with Equation (17). And the individual refrigerating COP of the HT cycle with Equation (18).

$$\dot{Q}_{O,H} = \dot{m}_{ref,H} \cdot \left[\frac{\left(h_{C1,O,o,H} - h_{C1,O,i,H}\right) + \left(h_{C2,O,o,H} - h_{C2,O,i,H}\right)}{2} \right] \tag{16}$$

$$\dot{Q}_{K,H} = \dot{m}_{ref,H} \cdot \left(h_{k,i,H} - h_{k,o,H}\right) \tag{17}$$

$$COP_H = \frac{\dot{Q}_{O,H}}{P_{C,H}} \tag{18}$$

Finally, refrigerating COP of the whole plant is evaluated with Equation (19), which considers the cooling capacity of the plant, Equation (12), the electrical power consumption of both compressors and of the fan of the gas-cooler (75 W).

$$COP = \frac{\dot{Q}_{O,L}}{P_{c,L} + P_{c,H} + P_{gc}} \tag{19}$$

The heat transfer rates of the secondary fluids are also calculated: in the LT evaporator with Equation (20) and in the HT condenser with Equation (21). Tyfoxit properties provided by the manufacturer [20] are used and water properties are evaluated with Refprop 9.1. These heat transfer rates are used for data validation.

$$\dot{Q}_{sf} = \dot{V}_{sf} \cdot \rho_{sf} \cdot c_{p,sf} \cdot \left(T_{sf,i} - T_{sf,o}\right) \tag{20}$$

$$\dot{Q}_{w} = \dot{V}_{w} \cdot \rho_{w} \cdot c_{p,w} \cdot \left(T_{w,o} - T_{w,i}\right) \tag{21}$$

4. Experimental procedure and data validation

4.1 Experimental procedure

The test campaign used to evaluate the performance of the cascade refrigeration system covered LT evaporating temperatures from -40 to -30 ºC and HT condensing temperatures from 30 to 50 ºC, those values regulated and maintained by the secondary fluid loop systems. For each combination of temperatures (9 tests), the operation of the cascade was registered at five LT condensing temperatures regulating the HT compressor speed. The LT compressor speed was maintained at its nominal value, as explained before. Tests were done fixing a degree of superheat in the valves of the R134a cascade condensers and of the CO_2 evaporator at 10 ºC. Also, the fan of the gas-cooler was always kept on, that consuming a constant value of 75 W.

In total, 45 steady-states of the plant were measured, each lasting at least 20 minutes, with 5 seconds sampling rate, with maximum oscillation of the phase-change temperatures of 2 %, as detailed in Table 2.

Additionally, two additional tests were carried out to analyze the performance of the compressors under speed variation. In these test, the compression rates were kept constant while varying the compressor's speed.

4.2 Data validation

Data validation was done comparing the heat transfer rates in the main heat exchangers of the plant. In Figure 3, we represent in red dots the heat transfer rate of water, Equation (21), versus the heat rejection of R134a in the HT condenser, Equation (17); in green diamonds the heat rejection of CO_2 , Equation (12), versus the cooling capacity of R134a in the cascade heat exchangers Equation (16); and in blue squares the heat transfer rate of the secondary fluid, Equation (20), versus the cooling capacity of CO_2, Equation (12), in the LT evaporator.

Regarding the heat balance at the HT condenser 99.6 % of values present a deviation below ±10 %, at the cascade heat exchanger 97.0 % of data are inside ±10 %, and data in the LT evaporator 92.4 % deviates less than ±10 %.

Figure 3. Validation of heat transfer rates in the cascade plant

5. Experimental results

A detailed energy balance of the cascade plant for a given operating condition is given in section 5.1, the compressors' performance is discussed in section 5.2 and the global performance of the plant over a wide range of operating conditions is analyzed in section 5.3.

5.1 Energy balance of the cascade plant

For clear understanding of the operation of the cascade refrigeration plant, the temperature-entropy diagram of both refrigeration cycles is presented in Figure 4, where the allocation of all measurement points in the plant is reflected (Figure 2). Also, in Figure 5, the energy flows through the cascade plant are detailed. Both figures represent the operation of the plant a LT evaporating temperature of -29.98 ºC, a HT condensing temperature of 40.08 ºC for compressors' speeds of 1450 rpm in the LT compressor and 806.4 rpm in the HT compressor. For this condition, the COP of the cascade plant is of 1.42.

LT cycle absorbs heat in the evaporator ($\dot{Q}_{O,L}$) and through the suction line ($\dot{Q}_{suc,L}$), this last accounting for less than 1 % of the cooling capacity. It consumes electricity in the CO_2 compressor ($\mathrm{P}_{c,L}$) and in the fan of the gas-cooler ($\mathrm{P}_{gc,L}$), this last accounting for 3.6 % of the total consumption of the LT cycle. The cycle rejects energy in the cascade condenser ($\dot{Q}_{K,L}$), through the discharge line ($\dot{Q}_{dis,L}$) and in the gas-cooler ($\dot{Q}_{gc,L}$), this last meaning 15.3 % of the total heat rejection. It is worth highlighting the objective of the gas-cooler. If environment temperature allows it, the gas-cooler rejects heat to the environment, thus avoiding pumping it to the condensing temperature of the HT cycle. This way the COP of the plant improves. The individual refrigerating COP of the LT cycle for this condition is of 3.10.

HT cycle absorbs heat in the cascade condenser ($\dot{Q}_{O,H}$) and in the suction line ($\dot{Q}_{suc,H}$), this last accounts for 1.2 % of the heat taken by the cycle. About electricity consumption, it absorbs energy in the R134a compressor ($\mathrm{P}_{C,H}$). Cycle rejects heat in the HT condenser ($\dot{Q}_{K,H}$) and through the discharge line ($\dot{Q}_{dis,H}$), this last means 6.9 % of the total heat rejection. The individual refrigerating COP of the HT is of 2.84.

Figure 4. Temperature-entropy of the cascade plant
at $TO_{,L}$ = -29.98 ºC, $TK_{,H}$ = 40.08 ºC, NL = 1450 rpm, NH = 806.4 rpm

Figure 5. Energy flow through the cascade plant
at $TO_{,L}$ = -29.98 ºC, $TK_{,H}$ = 40.08 ºC, NL = 1450 rpm, NH = 806.4 rpm

5.2 Compressors' performance

The way of modifying the intermediate conditions of the cascade cycle ($T_{K,L}$ or $T_{O,H}$) for a given operating condition ($T_{O,L}$ and $T_{K,H}$) is through the variation of the compressors speed, either of the LT compressor or the HT compressor. If for a constant N_H, N_L is increased, the LT cycle moves more refrigerant and the heat rejection at the cascade condenser increases, thus increasing $T_{K,L}$ and $T_{O,H}$, and obviously temperature difference in the cascade heat exchanger also increases. The same applies for variation of N_H.

Accordingly, to verify the best way to regulate the intermediate conditions, both compressors were subjected to a speed variation test under fixed compression ratios. Two individual tests were performed, one for each compressor, where their energy performance was evaluated. We summarize the test in Table 3.

In Figure 6, the evolution of the global efficiency is presented, Equations (8) and (9) (continuous line, left axis) and the discharge temperature (dashed line, right axis) of each compressor under speed variation for fixed compression ratios. Although both compressors are ready for variable speed operation, a big degradation of the global efficiency of the CO_2 compressor at low speeds was observed (5.2 % of reduction each 100 rpm in average), which consequence was an increase of the discharge temperature (from 80 to 122 ºC). This last effect is associated to the refrigeration of the electrical motor of the compressor, as analysed for another CO_2 compressor by Sánchez et al. [21]. About R134a compressor, efficiency variation with the speed is observed, but more soft (0.9 % of reduction each 100 rpm). Accordingly, the experimental evaluation of the cascade plant was carried out fixing N_L at the nominal design condition of the LT compressor (1450 rpm) and N_H was varied to modify the intermediate conditions.

Figure 6. Global efficiency of the compressors and discharge temperature vs. compressor's speed (fixed compression ratios)

In Figure 7, the global efficiencies of both compressors versus the compression ratio are presented, and in Equations (22) and (23) the adjusted polynomials for the global efficiency of the CO_2 (at 1450 rpm) and R134a compressors respectively, of all experimental data presented in Table 2. We observe the performance of CO_2 compressor is more dependent to the compression ratio than that of R134a one.

$$\eta_{G,L} = 0.7245 - 0.0852 \cdot t_L \quad (22)$$

$$\eta_{G,H} = 0.5871 - 0.01021 \cdot t_H + 6.067 \cdot 10^{-5} \cdot N_H \quad (23)$$

Figure 7. Compressors' efficiencies vs. compression ratio

5.3 Energy performance of the cascade refrigeration plant

Here, the measured performance of the cascade plant over a wide range of operating conditions is presented, as detailed in Table 2. In the test, the degrees of superheat in the heat exchangers were kept constant. The plant was evaluated at fixed operating conditions ($T_{O,L}$ and $T_{k,H}$), for constant N_L = 1450rpm, while varying the intermediate level through modification of N_H, as presented in Figure 8. In it, N_H was increased while maintaining constant $T_{O,L}$ and $T_{K,H}$. When N_H increases, the HT cycle provides more cooling capacity, the result being a decrease of the intermediate temperature level (for both $T_{K,L}$ and $T_{O,H}$). This modification of the intermediate level modifies the individuals COP (if N_H increases, COP_L increases and COP_H decreases) and the temperature difference in the cascade.

5.3.1 LT condensing temperature versus HT compressor speed

As mentioned, the way of modifying the intermediate conditions is through the variation of N_H. We present experimental measurements of the condensing temperature of the LT cycle ($T_{K,L}$) for the operation of the cascade plant at constant $T_{O,L}$ = -30 ºC for three $T_{K,H}$ values in Figure 9 and at constant $T_{K,H}$ = 40 ºC for three $T_{O,L}$ in Figure 10. From the results, we observe the variations of $T_{K,L}$ versus N_H are similar in both variation tests, with an average slope of -1.3 ºC for each 100 rpm increment. Regarding the modification of $T_{O,L}$ (Figure 10), $T_{K,L}$ increases 2.5 ºC for an increment of 5 ºC of the $T_{O,L}$. Nonetheless, when we modify $T_{K,H}$ (Figure 9), the increments of $T_{K,L}$ are not uniform, it increases 2 ºC when $T_{K,H}$ rises from 30 to 40 ºC and 3 ºC when $T_{K,H}$ increases from 40 to 50 ºC. Equation (24) represents the dependence of the LT condensing temperature in (ºC) with N_H, $T_{K,H}$ and $T_{O,L}$ adjusted from the experimental data.

$$T_{K,L} = 14.3617207 - 0.0111471 \cdot N_H + 0.2922665 \cdot T_{K,H} + 0.6279067 \cdot T_{O,L} \quad (24)$$

Figure 8. Phase-change temperatures vs. NH (at $TO_{,L}$ = -30 ºC, $Tk_{,H}$ = 40 ºC, NL = 1450 rpm)

Figure 9. LT condensing temperature vs. HT compressor speed ($TO_{,L}$ = -30 ºC)

Figure 10. LT condensing temperature vs. HT compressor speed ($TK_{,H}$ = 40 ºC)

5.3.2 Temperature difference in the cascade heat exchanger

Modification of N_H causes variations of the compression ratios, refrigerant mass flow rates, and energy parameters in each single-stage cycle. When N_H is increased, the cooling capacity of the HT cycle rises, and it modifies the temperature difference in the cascade heat exchanger (ΔT_{casc}), Equation (5). We present the experimental evolutions of ΔT_{casc} for constant operation of the cascade at $T_{O,L}$ = -30 ºC in Figure 11 and for constant operation at $T_{K,H}$ = 40 ºC in Figure 12. We observe the increase of N_H negatively affects ΔT_{casc}. The increase of $T_{K,H}$ affects ΔT_{casc} (Figure 11), but its variation is small, approximately 0.7 ºC increase of ΔT_{casc} when $T_{K,H}$ rises from 30 to 50 ºC. However, variation of $T_{O,L}$ (Figure 12) has greater influence on ΔT_{casc}, we measured an increment of 0.5 ºC when $T_{O,L}$ drops from -30 to -35 ºC and of 0.8 ºC when it drops from -35 to -40 ºC. Equation (25) represents the dependence of the ΔT_{casc} in (ºC) with N_H, $T_{K,H}$ and $T_{O,L}$ adjusted from the experimental data.

$$\Delta T_{casc} = -1.5858839 + 0.0025688 \cdot N_H + 0.0348272 \cdot T_{K,H} - 0.0515079 \cdot T_{O,L} \qquad (25)$$

Figure 11. Cascade temperature difference vs. HT compressor speed ($TO_{,L}$ = -30 ºC)

Figure 12. Cascade temperature difference vs. HT compressor speed ($Tk_{,H}$ = 40 ºC)

5.3.3 Cooling capacity

The experimental cooling capacity provided by the plant, Equation (12), at constant $T_{O,L}$ = -30 ºC is presented in Figure 13 and at constant $T_{K,H}$ = 40 ºC in Figure 14. For this representation we select the condensing temperature of the LT cycle for better understanding, as selected previously by other authors [12]. First and regarding $T_{K,L}$, we observe the capacity of the cascade plant reduces linearly when the inter-stage level increases. This effect is caused by the reduction of the refrigerant mass flow rate through the LT cycle. Although the COP of the plant can improve when $T_{K,L}$ increases (section 5.3.4), its increase always implies an increment of the low-stage compression ratio (t_L), which consequence is a reduction of the refrigerant mass flow rate through the LT cycle. About the dependence of the capacity on the external conditions, we observe the capacity of the cascade is much more dependent on the evaporating level ($T_{O,L}$, Figure 14) than on the condensing one ($T_{K,H}$, Figure 13). The reason is that when we modify $T_{K,H}$ the states of the refrigerant in the LT cycle remain practically constant, whereas when we vary $T_{O,L}$ the

modifications directly affect the states of the refrigerant at the LT compressor suction. Obviously, we can affirm that the capacity of the cascade is not much dependent on the environment temperature.

Figure 13. Cooling capacity vs. LT condensing temperature ($TO_{,L}$ = -30 ºC)

Figure 14. Cooling capacity vs. LT condensing temperature ($Tk_{,H}$ = 40 ºC)

5.3.4 COP

The evaluated COP of the cascade plant, Equation (19), for operation at $T_{O,L}$ = -30 ºC is presented in Figure 15 and for $T_{K,H}$ = 40 ºC in Figure 16. About the COP, we observe it is dependent on the condensing temperature of the LT cycle, it improves when $T_{K,L}$ increases. It seems that a maximum COP exists for a given $T_{K,L}$, as analyzed theoretically by other authors [8, 22] and verified experimentally for a NH_3/CO_2 cascade [12], however in our plant we could not reach an optimum value apparently. The last experimental point we could measure for each test condition (the one at the maximum $T_{K,L}$ in each line) was the limit of the CO_2 compressor previous to the activation of the thermal protection of the compressor. Nonetheless, we observe that the COP dependence on $T_{K,L}$ is not much significant, since over all the range of variation of $T_{K,L}$ the maximum COP variation we measured was of 6 %. Regarding COP dependence on $T_{K,H}$ (Figure 15), we observe the cascade presents an average reduction of 18 % for each 10 ºC increment of this temperature. On the other side, COP dependence on $T_{O,L}$, we observe a COP reduction of 12 % in average for each reduction of 5 ºC of this temperature (Figure 16).

Figure 15. COP vs. LT condensing temperature ($TO_{,L}$ = -30 ºC)

Figure 16. COP vs. LT condensing temperature ($Tk_{,H}$ = 40 ºC)

5.3.5 Discharge temperature of the CO_2 compressor

Finally, the measurements of the discharge temperature of the CO_2 compressor for constant $T_{O,L}$ = -30 ºC are presented in Figure 17 and for constant $T_{K,H}$ = 40 ºC in Figure 18. About the influence of $T_{K,L}$, we observe the discharge temperature rises linearly with $T_{K,L}$ at an average ratio of increase of $T_{dis,L}$ of 3 ºC for 1 ºC increment of $T_{K,L}$. About the external conditions, $T_{K,H}$ does not affect to the discharge temperature (Figure 17) but $T_{O,L}$ strongly affects this value (Figure 18). We measured in average increments of 20 ºC in $T_{dis,L}$ when $T_{O,L}$ increased 5 ºC.

As mentioned in the description of the plant, when the discharge temperature of the CO_2 compressor is higher than the environment temperature (in all tests in our experimental evaluation), it is recommended to reject heat in the LT cycle previous entering to the cascade heat exchanger for improving COP (Figure 2 and Figure 5). In our measurements, the gas-cooler of the plant extracted between 0.8 to 1.4 kW.

Figure 17. LT discharge temperature vs. LT condensing temperature ($TO_{,L}$ = -30 ºC)

Figure 18. LT discharge temperature vs. LT condensing temperature ($TK_{,H}$ = 40 ºC)

6. Conclusions

This work presents the experimental evaluation of a R134a/CO_2 cascade refrigeration plant driven by two semi-hermetic compressors designed to operate at the low evaporating temperature level of commercial refrigeration. The plant, fully instrumented, allows measuring its experimental energy performance. Here, we analysed the plant over a wide range of operating conditions, evaporating levels from -40 to -30 ºC, condensing levels from 30 to 50 ºC with variation of the condensing temperature of the low-temperature cycle.

It was observed the performance of the compressors was different when subjected to variations of speed. While the R134a compressor presented a small improvement when the speed increased, the CO_2 compressor presented low efficiencies at speeds below the nominal point. However, at nominal conditions the performance of the CO_2 compressor was similar to that of R134a one. We observed a quick decrease of efficiency of CO_2 compressor at high compression ratios.

In the plant we modified the intermediate level, condensing temperature of the low-temperature cycle, with speed variation of the high-temperature compressor. It was observed a negative linear dependence of this temperature with the compressor speed. Also, when this speed increased, temperature difference in the cascade heat exchanger increased too, and this increment was more significant at low evaporating temperatures. The measured temperature differences in the cascade heat exchanger in the tests ranged from 3.3 to 5.3 ºC.

About the energy performance, it was observed the cooling capacity is negatively linear dependent with the condensing temperature of the low-temperature cycle, and it is not much affected with variations of the high condensing temperature, but its changes are very significant when subjected to modifications of the low evaporating temperature. The measured cooling capacities ranged from 7.5 kW at an evaporating temperature of -30 ºC at a condensing of 30 ºC to 4.5 kW at -40 ºC and 40 ºC. About refrigerating COP, and inside the test range, it was observed a dependence of this parameter with the condensing temperature of the low temperature cycle, increasing COP when rising the condensing temperature. An optimum condensing temperature of the low temperature cycle could not be measured, if it existed, it was placed out of the application range of the LT cycle. Nonetheless, variations of COP for a given external condition with this temperature were below 6 %. The measured COP ranged from 1.05 at -40 and 40 ºC to 1.65 at -30 and 30 ºC. We measured reductions of COP of 18 % when the high condensing temperature increased 10 ºC and reductions of 12 % for each 5 ºC reduction of the low evaporating temperature.

Finally, it was observed in the experimental measurements discharge temperatures of the CO_2 compressor higher than the environment temperature, which brings the possibility of using a gas-cooler to

reject heat in the low temperature cycle before entering the cascade condenser, which improves the COP of the plant.

7. Acknowledgements

The authors gratefully acknowledge Jaume I University of Spain, who financed the present study through the research project P1·B2013-10.

8. References

[1] D. Cowan, J. Gartshore, I. Chaer, C. Francis, G. Maidment, REAL ZERO - reducing refrigerant emissions & leakage - feedback from the IOR project, Proceedings of the Institute of Refrigeration, 2009-10. 7-1 (2010).

[2] Arias J., Energy Usage in Supermarkets - Modelling and Field Measurements, in: Department of Energy Technology, Royal Institute of Technology, Sweden, 2005.

[3] European Commission, Regulation (EU) No 517/2014 of the European Parliament and of the Council of 16 April 2014 on fluorinated greenhouse gases and repealing Regulation (EC) No 842/2006., (2014).

[4] UNEP, 2010 Report of the Refrigeration, Air Conditioning and Heat Pumps Technical Options Committee (RTOC), 2010 Assessment, in, 2011.

[5] J.M. Calm, G.C. Hourahan, Physical, safety, and environmental data for current and alternative refrigerants, in: I.I.o. Refrigeration (ed.) 23rd IIR International Congress of Refrigeration, IIR, Prage, 2011.

[6] T.S. Lee, C.H. Liu, T.W. Chen, Thermodynamic analysis of optimal condensing temperature of cascade-condenser in CO_2/NH_3 cascade refrigeration systems, International Journal of Refrigeration, 29 (2006) 1100-1108.

[7] A. Dopazo, J. Fernández-Seara, J. Sieres, F.J. Uhía, Theoretical analysis of a CO2-NH3 cascade refrigeration system for cooling applications at low temperatures, Applied Thermal Engineering, 29 (2009) 1577-1583.

[8] A. Messineo, R744-R717 Cascade Refrigeration System: Performance Evaluation compared with a HFC Two-Stage System, Energy Procedia, 14 (2012) 56-65.

[9] H.M. Getu, P.K. Bansal, Thermodynamic analysis of an R744-R717 cascade refrigeration system, International Journal of Refrigeration, 31 (2008) 45-54.

[10] J. Xiao, Y.F. Liu, Thermodynamic analysis of a R32/CO2 cascade refrigeration cycle, in, Vol. 732-733, Advanced Materials Research 2013, pp. 527-530.

[11] W. Bingming, W. Huagen, L. Jianfeng, X. Ziwen, Experimental investigation on the performance of NH_3/CO_2 cascade refrigeration system with twin-screw compressor, International Journal of Refrigeration, 32 (2009) 1358-1365.

[12] J.A. Dopazo, J. Fernández-Seara, Experimental evaluation of a cascade refrigeration system prototype with CO2 and NH3 for freezing process applications, International Journal of Refrigeration, 34 (2011) 257-267.

[13] A. da Silva, E.P. Bandarra Filho, A.H.P. Antunes, Comparison of a R744 cascade refrigeration system with R404A and R22 conventional systems for supermarkets, Applied Thermal Engineering, 41 (2012) 30-35.

[14] UNEP, Low-GWP alternatives in commercial refrigeration: propane, CO2 and HFO case studies. www.unep.org/ccac/portals/50162/docs/Low-GWP_Alternatives_in_Commercial_Refrigeration-Case_Studies-Final.pdf (29/06/2014), in, 2014.

[15] E. Torrella, R. Llopis, R. Cabello, Experimental evaluation of the inter-stage conditions of a two-stage refrigeration cycle using a compound compressor, International Journal of Refrigeration, 32 (2009) 307-315.

[16] R. Llopis, E. Torrella, R. Cabello, D. Sánchez, Performance evaluation of R404A and R507A refrigerant mixtures in an experimental double-stage vapour compression plant, Applied Energy, 87 (2010) 1546-1553.

[17] R. Llopis, E. Torrella, R. Cabello, D. Sánchez, HCFC-22 replacement with drop-in and retrofit HFC refrigerants in a two-stage refrigeration plant for low temperature, International Journal of Refrigeration, 35 (2012) 810-816.

[18] R. Cabello, R. Llopis, D. Sánchez, E. Torrella, REFLAB: An interactive tool for supporting practical learning in the educational field of refrigeration, International Journal of Engineering Education, 27 (2011) 909-918.

[19] E.W. Lemmon, M.L. Huber, M.O. McLinden, REFPROP, NIST Standard Reference Database 23, v.9.1. National Institute of Standards, Gaithersburg, MD, U.S.A., (2013).

[20] TYFO, High-performance low viscous secondary refrigerant for applications down to -55ºC. In: www.tyfo.de/uploads/TI/IT-TYFOXIT-F15-F50_es_2013.pdf (29/06/2014), in, 2013.

[21] D. Sánchez, E. Torrella, R. Cabello, R. Llopis, Influence of the superheat associated to a semihermetic compressor of a transcritical CO2 refrigeration plant, Applied Thermal Engineering, 30 (2010) 302-309.

[22] G. Di Nicola, F. Polonara, R. Stryjek, A. Arteconi, Performance of cascade cycles working with blends of CO2 + natural refrigerants, International Journal of Refrigeration, 34 (2011) 1436-1445.

FIGURES

Figure 1. View of the cascade refrigeration prototype

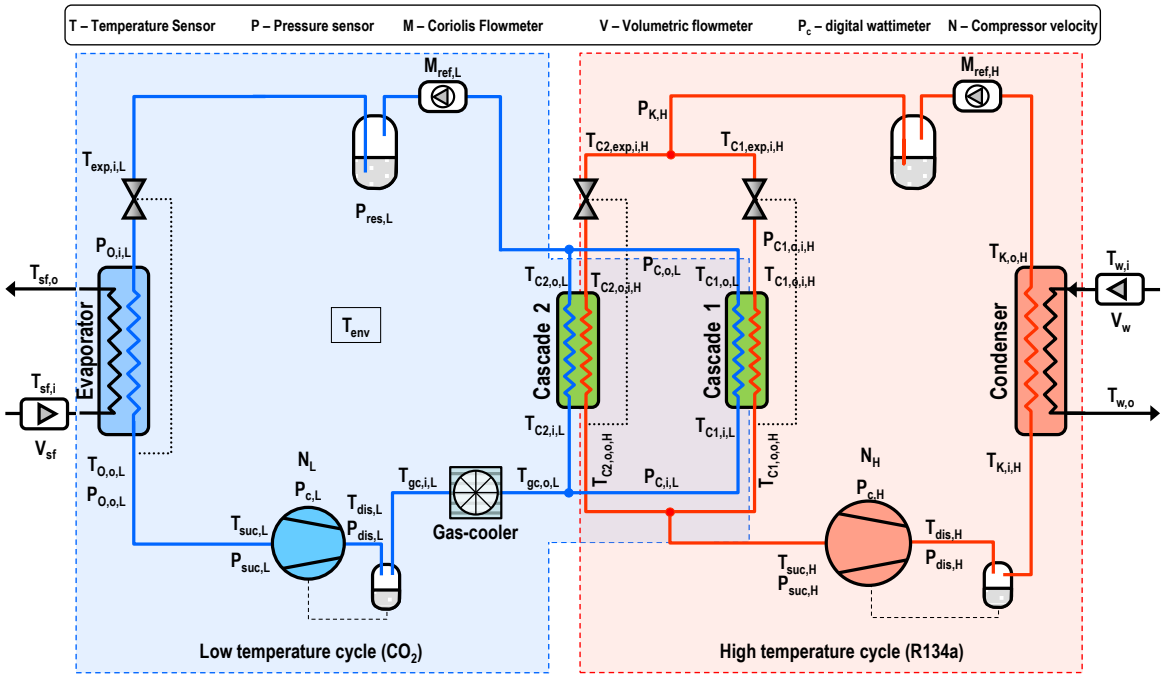

Figure 2. Schematic diagram of the experimental plant

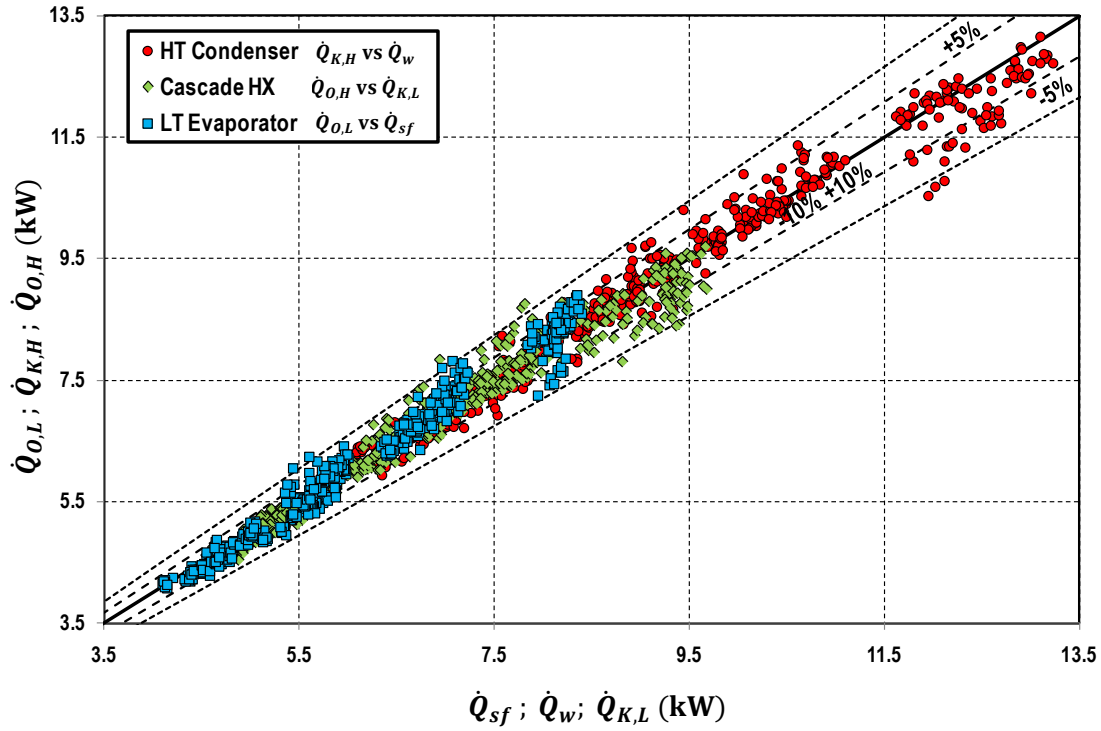

Figure 3. Validation of heat transfer rates in the cascade plant

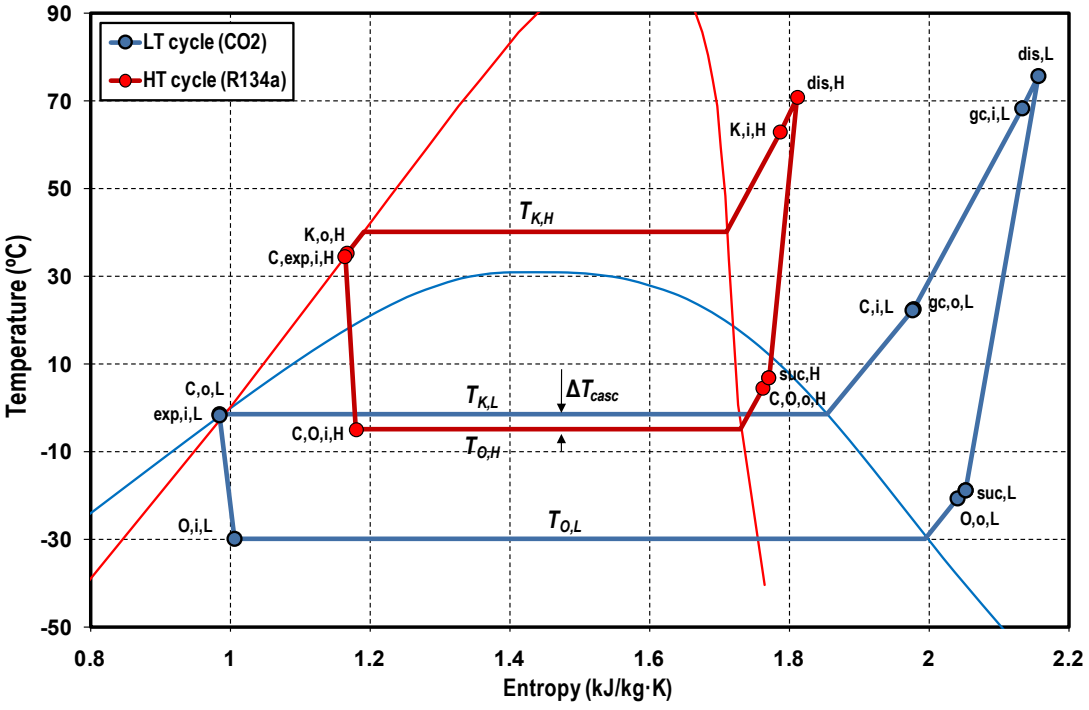

Figure 4. Temperature-entropy of the cascade plant

at $T_{O,L}$ = -29.98 ºC, $T_{K,H}$ = 40.08 ºC, N_L = 1450 rpm, N_H = 806.4 rpm

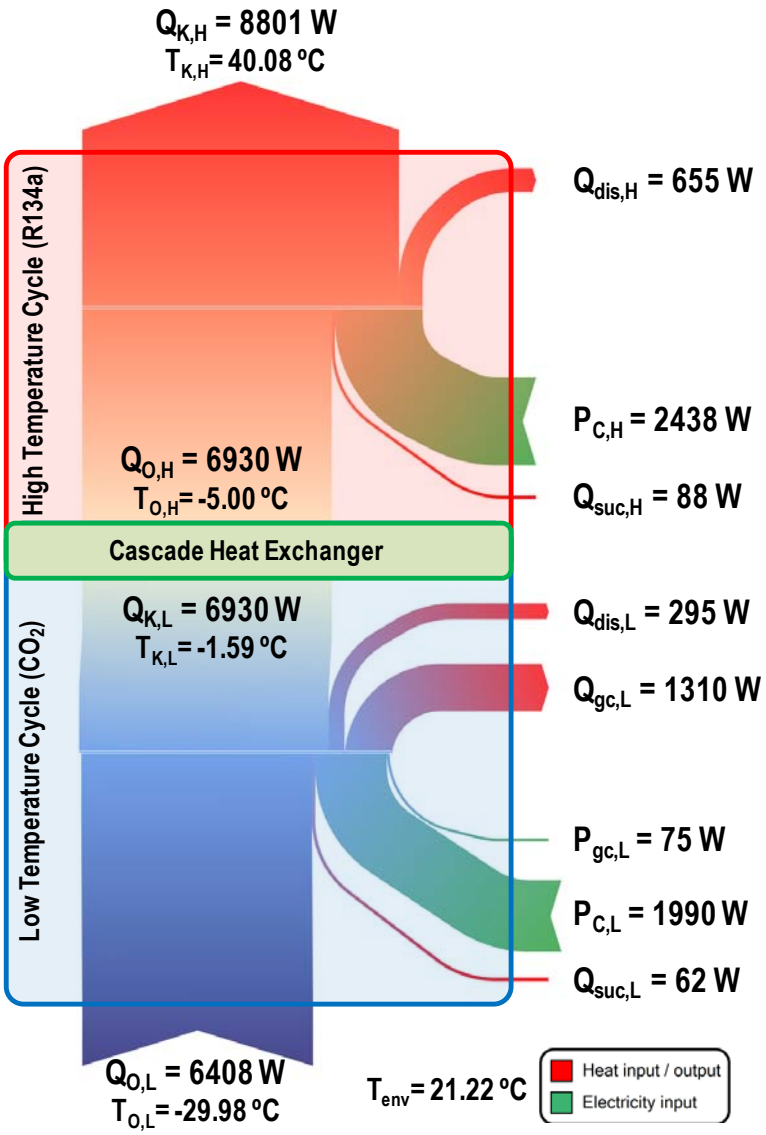

Figure 5. Energy flow through the cascade plant

at $T_{O,L}$ = -29.98 °C, $T_{K,H}$ = 40.08 °C, N_L = 1450 rpm, N_H = 806.4 rpm

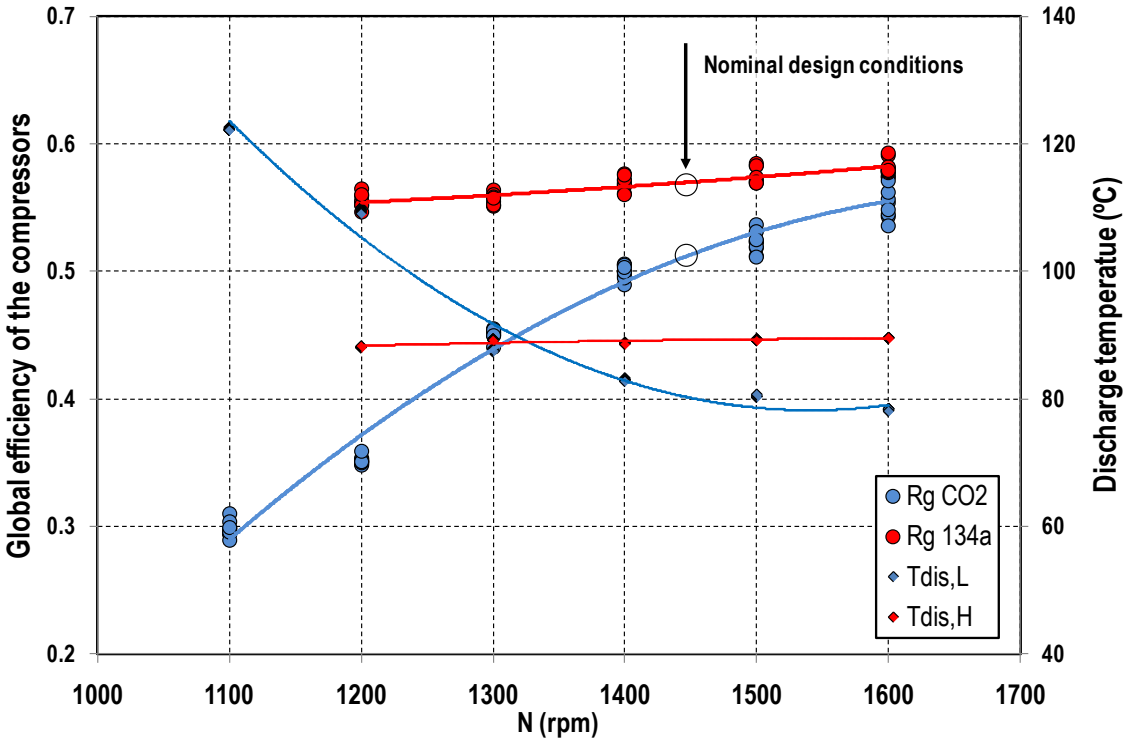

Figure 6. Global efficiency of the compressors and discharge temperature vs. compressor's speed (fixed compression ratios)

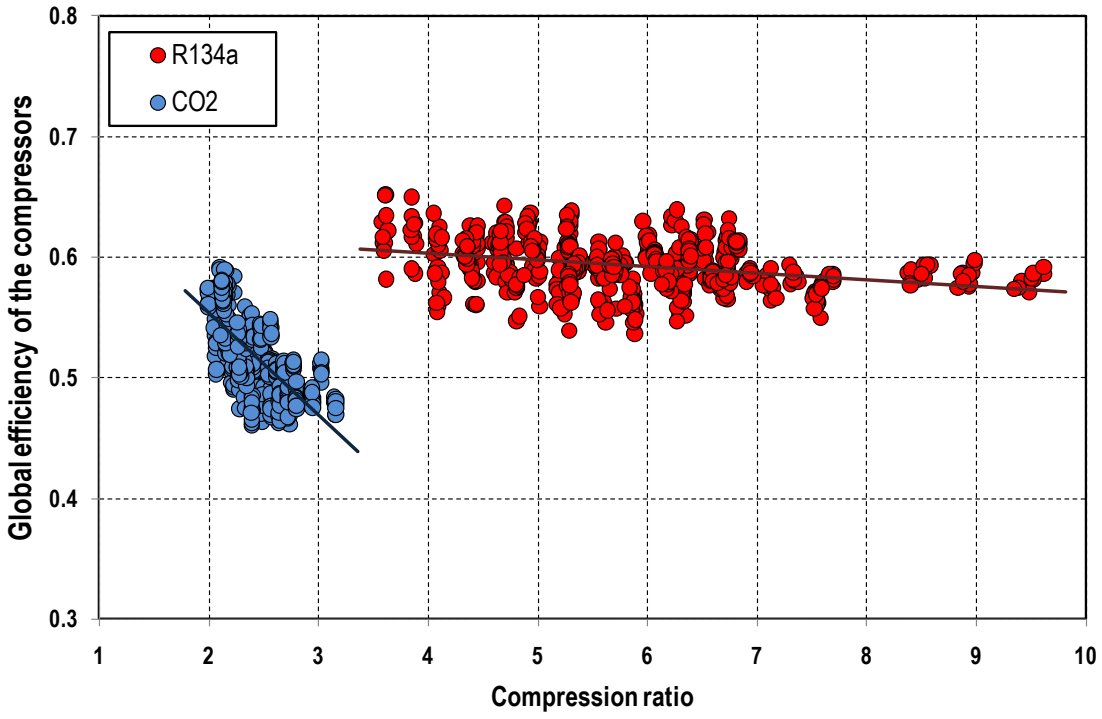

Figure 7. Compressors' efficiencies vs. compression ratio

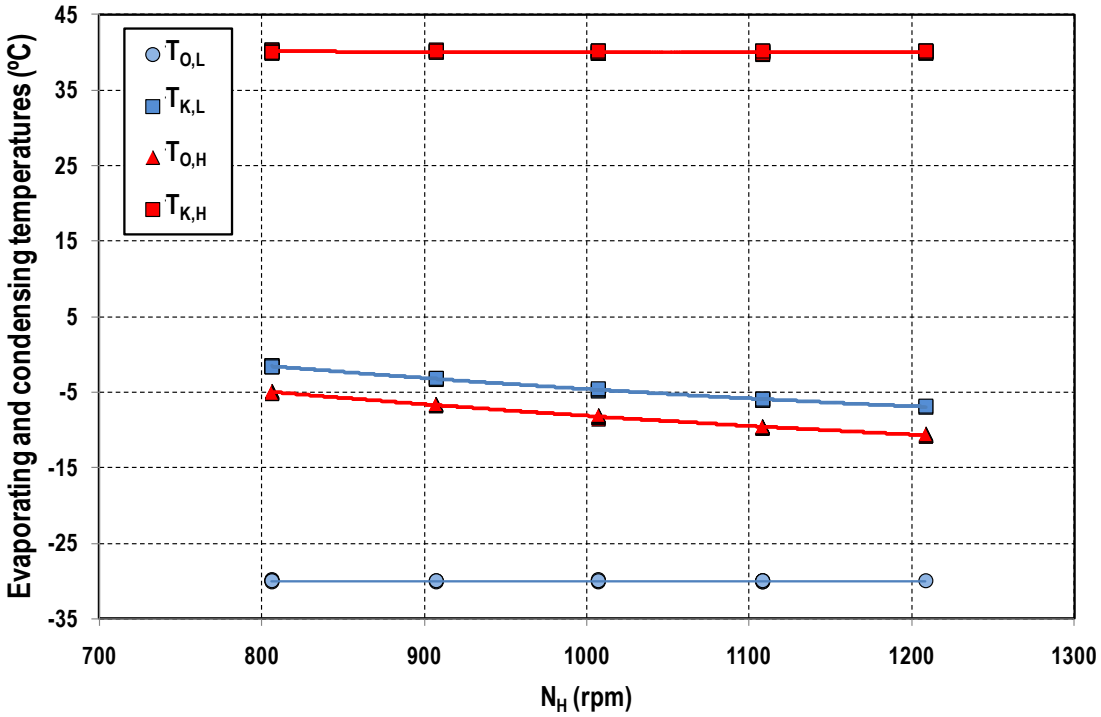

Figure 8. Phase-change temperatures vs. N_H (at $T_{O,L}$ = -30 ºC, $T_{k,H}$ = 40 ºC, N_L = 1450 rpm)

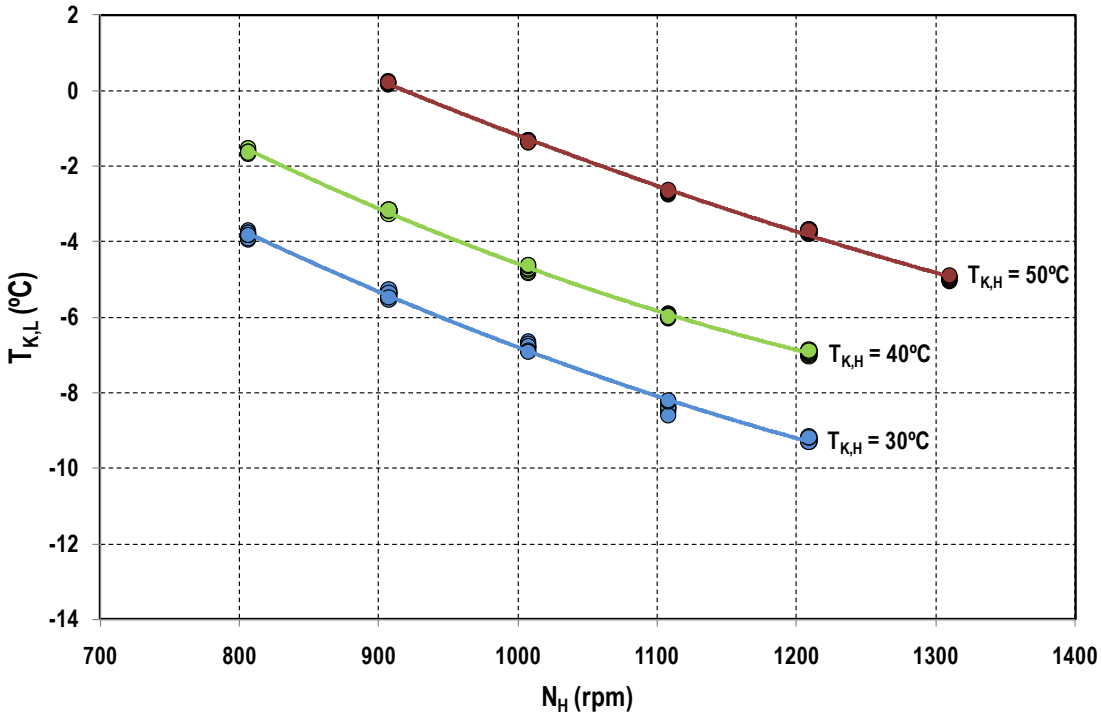

Figure 9. LT condensing temperature vs. HT compressor speed ($T_{O,L}$ = -30 ºC)

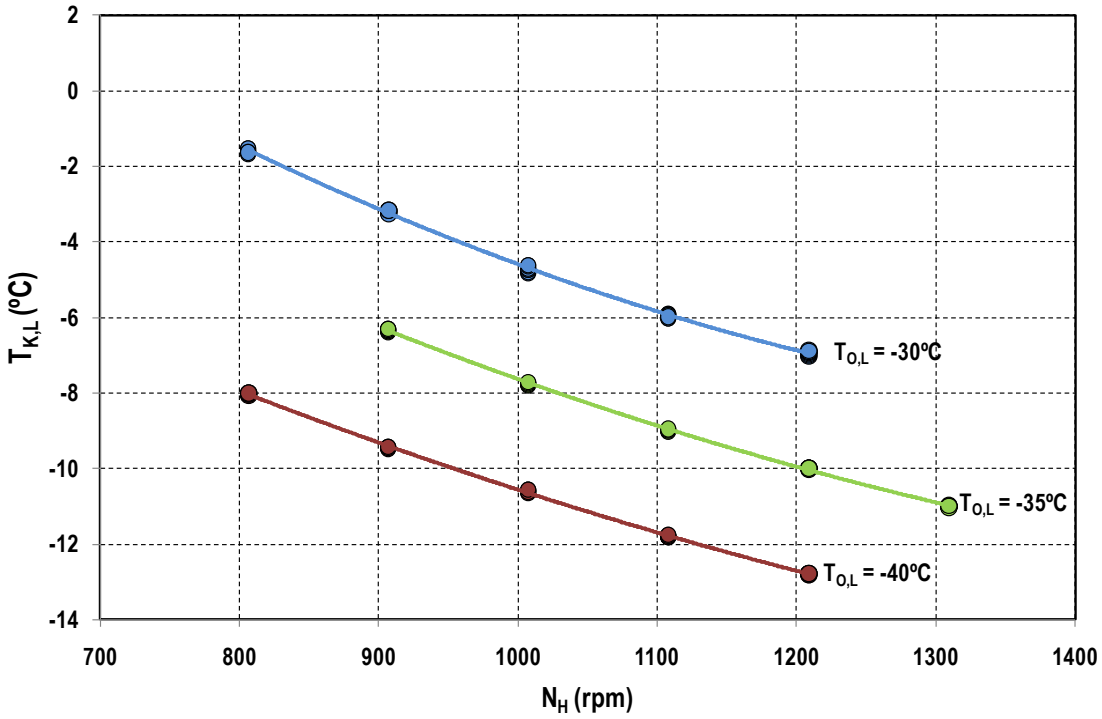

Figure 10. LT condensing temperature vs. HT compressor speed ($T_{K,H}$ = 40 ºC)

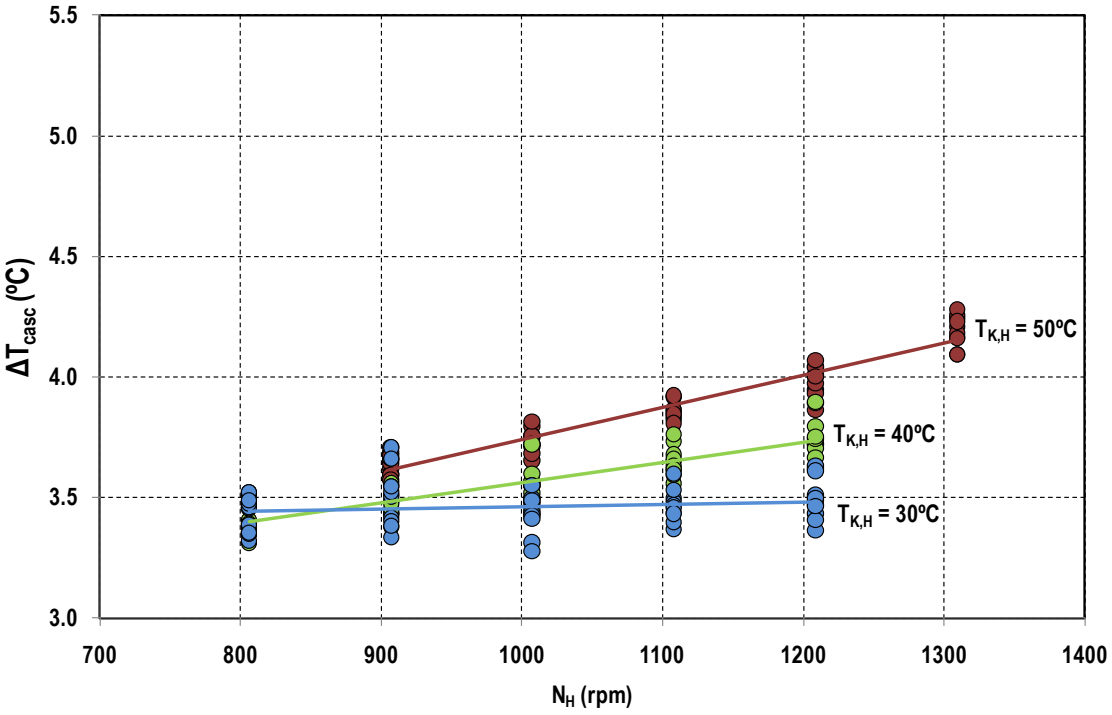

Figure 11. Cascade temperature difference vs. HT compressor speed ($T_{O,L}$ = -30 ºC)

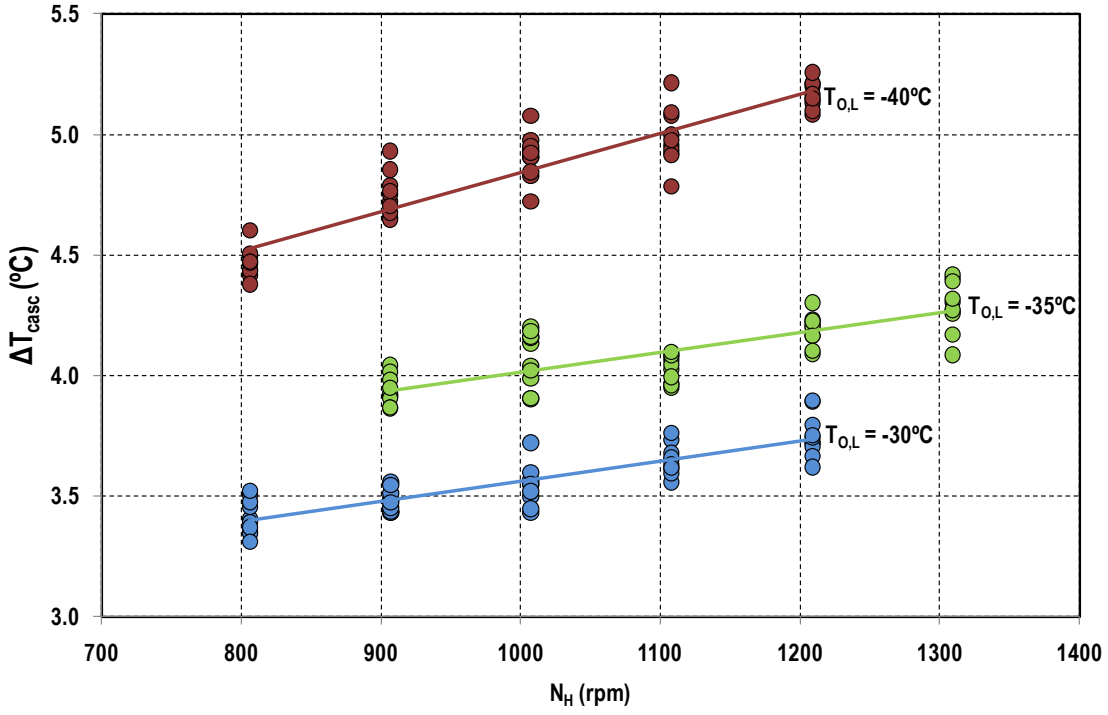

Figure 12. Cascade temperature difference vs. HT compressor speed ($T_{k,H}$ = 40 ºC)

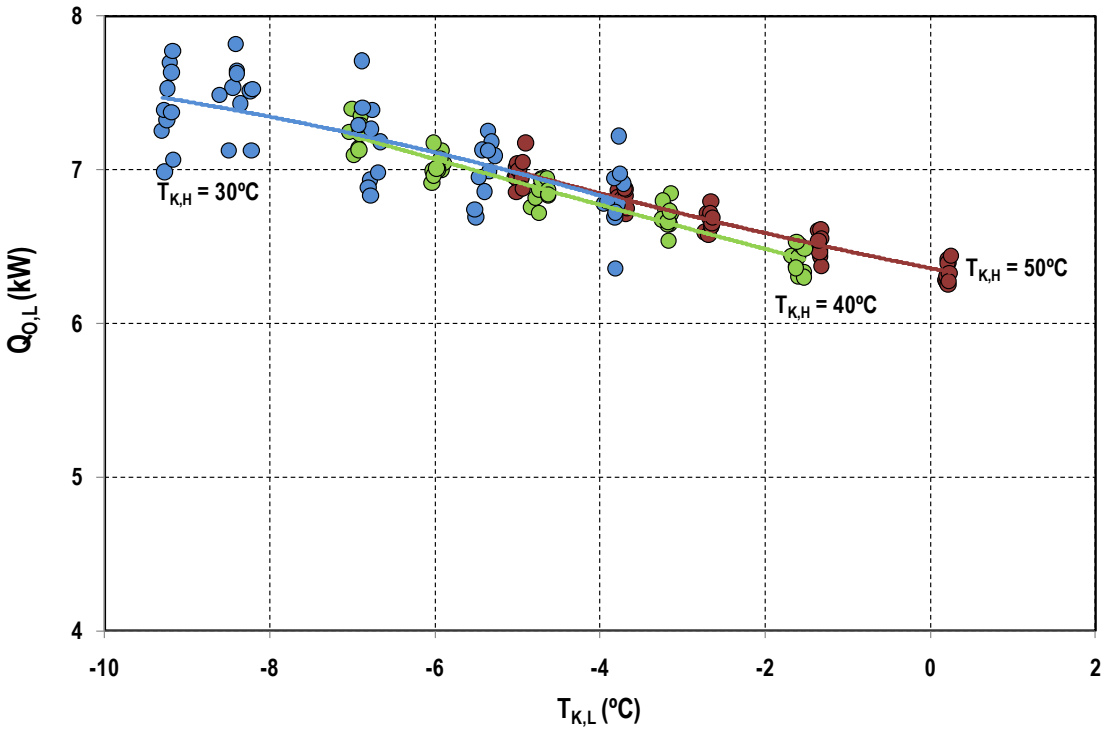

Figure 13. Cooling capacity vs. LT condensing temperature ($T_{O,L}$ = -30 ºC)

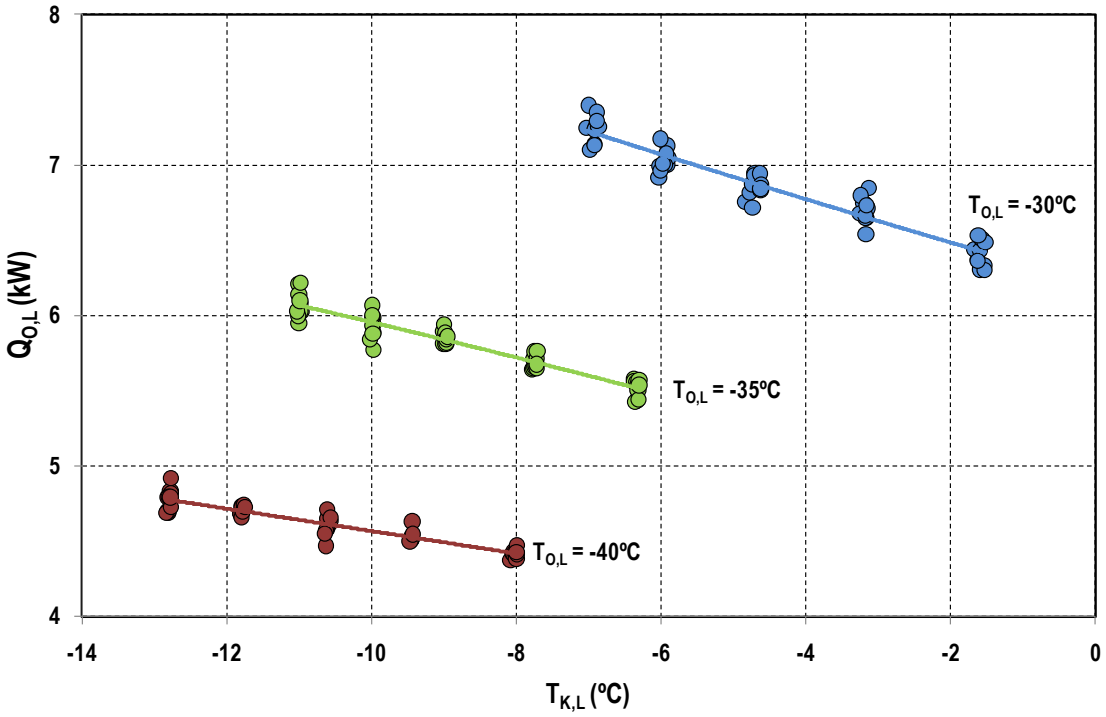

Figure 14. Cooling capacity vs. LT condensing temperature ($T_{k,H}$ = 40 ºC)

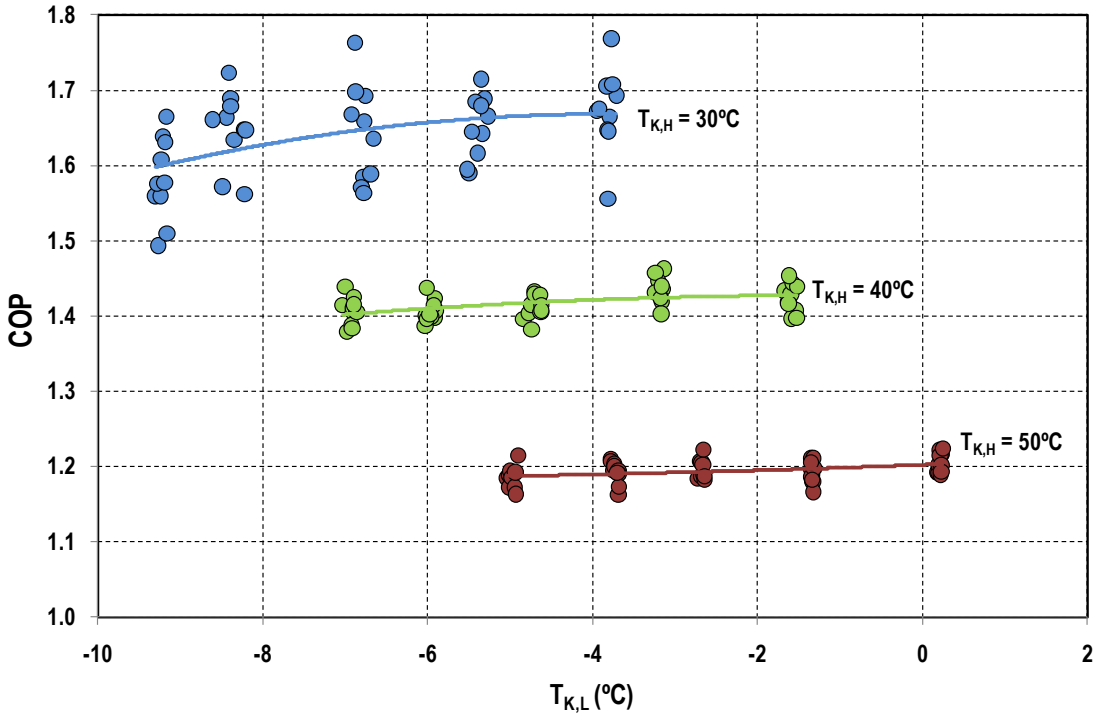

Figure 15. COP vs. LT condensing temperature ($T_{O,L}$ = -30 °C)

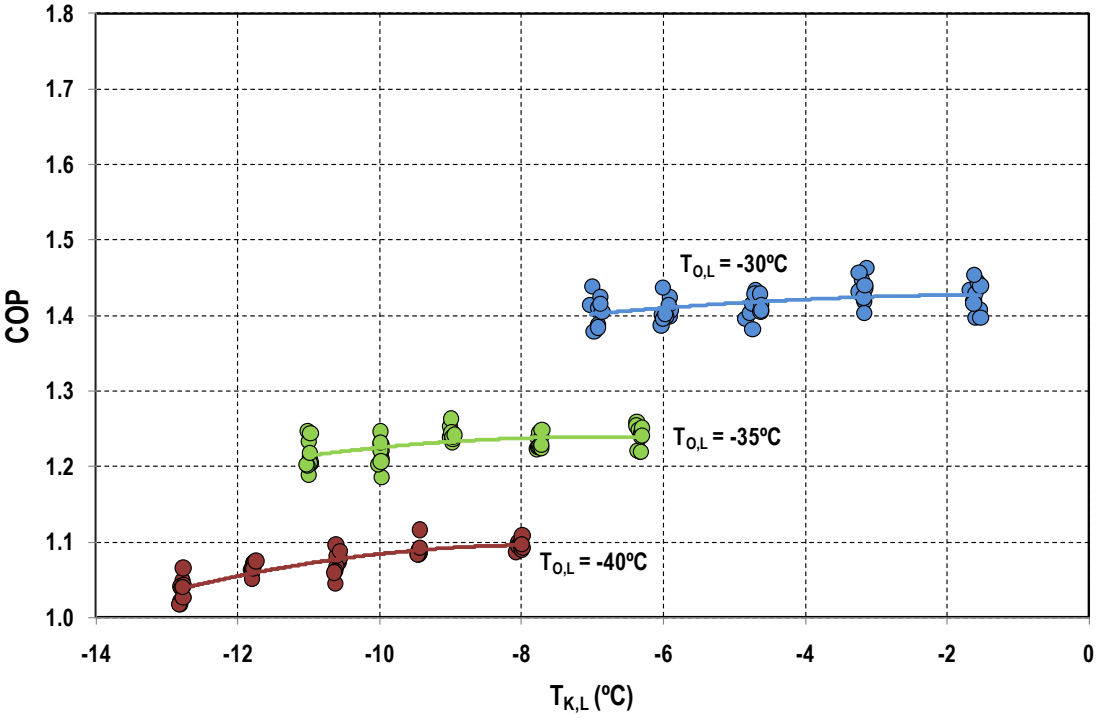

Figure 16. COP vs. LT condensing temperature ($T_{k,H}$ = 40 °C)

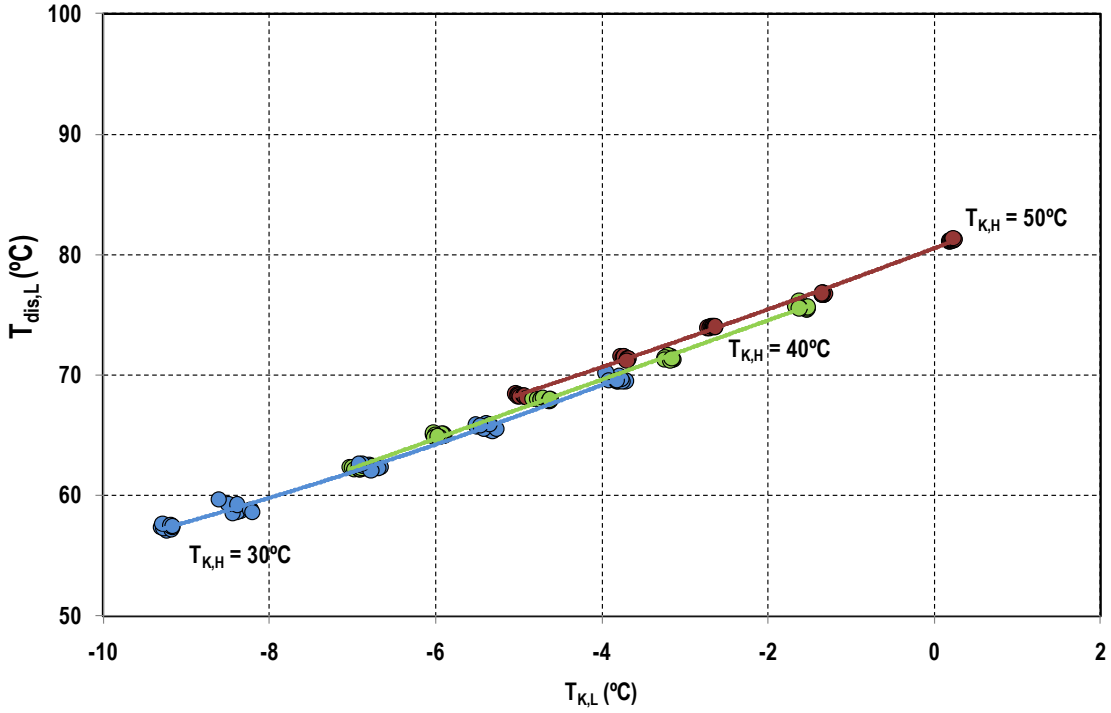

Figure 17. LT discharge temperature vs. LT condensing temperature ($T_{O,L}$ = -30 ºC)

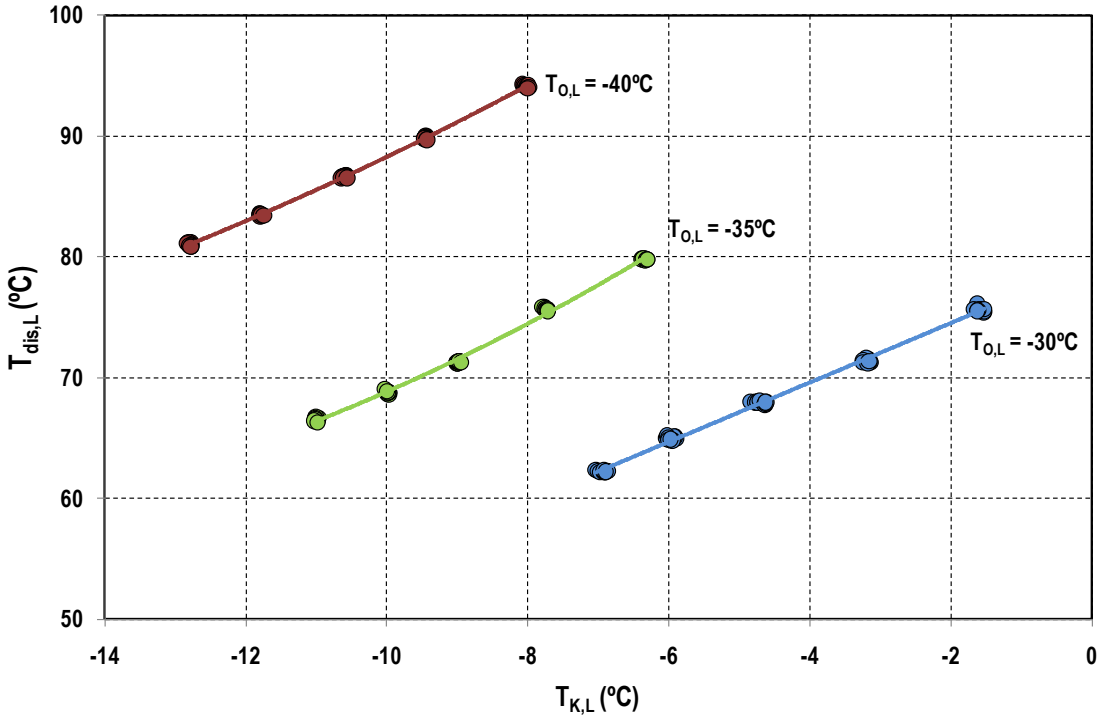

Figure 18. LT discharge temperature vs. LT condensing temperature ($T_{K,H}$ = 40 ºC)

TABLES

Table 1. Accuracies and calibration range of the transducers

Sensors	Measured variable	Measurement device	Calibration range	Calibrated accuracy
25	temperature	T-type thermocouple	-62 to 125 ºC	±0.5 ºC
3	low pressure LT cycle	piezoelectric gauge	0 to 60 bar	±0.18 bar
4	high pressure LT cycle	piezoelectric gauge	0 to 100 bar	±0.3 bar
2	low pressure HT cycle	piezoelectric gauge	0 to 10 bar	±0.03 bar
2	high pressure HT cycle	piezoelectric gauge	0 to 25 bar	±0.075 bar
1	LT mass flow rate	coriolis	8.5 $kg \cdot min^{-1}$	±0.15% of lecture
1	HT mass flow rate	coriolis	52.8 $kg \cdot min^{-1}$	±0.15% of lecture
2	SF volumetric flow rates	magnetic flow meter	0 to 4 $m^{3} \cdot h^{-1}$	±0.33% of lecture
2	compressor power consumption	digital wattmeter	0 to 6 kW	±0.5% of lecture
2	compressor speed	inverter drive signal	0 to1800 rpm	±1.3% of lecture

Table 2. Test summary of the cascade refrigeration plant evaluation

	$T_{O,L}$ (ºC)	$T_{K,L}$ (ºC)	$\Delta T_{SH,L}$ (ºC)	N_L (rpm)	$T_{O,H}$ (ºC)	$T_{K,H}$ (ºC)	$\Delta T_{SH,H}$ (ºC)	T_{env} (ºC)	N_H (rpm)	Steady-states
Test 1	-29.98 ± 0.05	--4.98 to 0.21	9.01 ± 0.26	1450	-9.17 to -3.43	50.07 ± 0.07	8.74 ± 0.82	27.54 ± 1.57	906.8 to 1309.6	5
Test 2	-35.00± 0.04	-6.66 to -0.35	9.03 ± 0.23	1450	-11.29 to -3.50	50.01 ± 0.07	10.04 ± 0.50	26.60 ± 0.92	704.7 to 1208.7	5
Test 3	-39.96 ± 0.02	-11.52 to -4.83	9.04 ± 0.22	1450	-17.10 to -9.52	49.96 ± 0.07	9.46 ± 1.85	24.31 ± 1.27	806.4 to 1409.4	5
Test 4	-30.01 ± 0.03	-6.93 to -1.59	9.44 ± 0.44	1450	-10.68 to -5.00	40.06 ± 0.04	9.51 ± 0.65	21.80 ± 1.3	806.4 to 1208.7	5
Test 5	-35.03 ± 0.06	-11.00 to -6.34	9.28 ± 0.27	1450	-15.29 to -10.28	40.05 ± 0.09	9.43 ± 0.46	21.39 ± 1.40	906.8 to 1309.6	5
Test 6	-40.03 ± 0.03	-12.80 to -8.02	9.32 ± 0.07	1450	-17.96 to -12.49	40.07 ± 0.05	9.65 ± 0.44	20.68 ± 0.69	806.4 to 1208.7	5
Test 7	-30.05 ± 0.12	-9.23 to -3.82	9.31 ± 1.08	1450	-12.71 to -7.25	30.17 ± 0.14	10.49 ± 1.19	22.75 ± 0.71	806.4 to 1208.7	5
Test 8	-34.94 ± 0.05	-12.17 to -7.23	9.48 ± 0.40	1450	-16.03 to -10.57	29.97 ± 0.07	9.67 ± 1.09	20.98 ± 1.39	806.4 to 1208.7	5
Test 9	-40.04 ± 0.05	-15.36 to -10.27	9.39 ± 0.07	1450	-20.15 to -14.43	30.07 ± 0.06	9.43 ± 0.90	19.99 ± 1.13	806.4 to 1208.7	5

Table 3. Test summary of compressors' evaluation

	P_{suc} (bar)	P_{dis} (bar)	t_L (-)	T_{suc} (ºC)	N (rpm)	m_{ref} (kg/s)	P_C (kW)	η_G (-)	T_{dis} (ºC)	Steady-states
LT Comp test	11.78 ± 0.11	27.44 ± 0.45	2.33 ± 0.06	-12.46 ± 0.51	1100 to 1600	0.013 to 0.024	1.66 to 1.83	0.29 to 0.57	78.0 to 122.6	6
HT Comp test	1.24 ± 0.01	10.18 ± 0.04	8.23 ± 0.09	-4.71 ± 0.48	1200 to 1600	0.031 to 0.045	2.71 to 3.63	0.70 to 0.77	88.0 to 89.6	5